**Title:** Highly sensitive *in vivo* detection of dynamic changes in enkephalins following acute stress

**Authors:** Marwa O. Mikati[1,2,3], Petra Erdmann-Gilmore[4], Rose Connors[4], Sineadh M. Conway[1,2,3], Jim Malone[4], Justin Woods[1,2,3], Robert W. Sprung[4], R. Reid Townsend[4], Ream Al-Hasani [1,2,3].

[1]Department of Anesthesiology, [2]Washington University Pain Center, Washington University in St. Louis, MO, USA; [3]Center for Clinical Pharmacology, University of Health Science and Pharmacy in St. Louis, MO, USA, [4]Department of Medicine, Washington University School of Medicine, Washington University in St. Louis, St. Louis, MO, USA

**Correspondence:** Ream Al-Hasani, PhD: al-hasanir@wustl.edu.

**Abstract:** Enkephalins are opioid peptides that modulate analgesia, reward, and stress. *In vivo* detection of enkephalins remains difficult due to transient and low endogenous concentrations and inherent sequence similarity. We present an analytical method for Met- and Leu-Enkephalin detection in the mouse Nucleus Accumbens shell after acute stress. This approach increases spatiotemporal resolution, optimizes the detection of Met-Enkephalin through methionine oxidation, and provides insight into the relationship between Met- and Leu-Enkephalin following stress.

**Main**

Endogenous opioid peptides are released at significantly lower concentrations than small molecule neurotransmitters and undergo post-translational processing that yields ~30 unique peptides from 4 precursor molecules. Together, these properties have made sensitive peptide detection difficult to achieve with existing technologies [1]. Here, we describe an analytical method that enables quantification of dynamic *in vivo* changes in both Leu- and Met-enkephalin (Leu-Enk and Met-Enk) peptides in rodents. We show unique release profiles between Leu- and Met-Enk in response to two different stressors and gain new insight into peptide release dynamics; additionally, our method offers improved spatiotemporal resolution. More broadly, this approach will enable an understanding of how neuropeptide levels change in response to acute or chronic behavioral, pharmacological, and neurophysiological manipulations.

Enkephalins can act on both the delta and/or mu opioid receptors, but their activity often depends on receptor and peptide expression patterns, which differ across the brain [2–5]. Confirming an opioid peptide's identity based on the activity of the receptor alone poses difficulties. For example, in a single brain region, the mu opioid receptor may be activated by an enkephalin or endorphin peptide [3]. It has been particularly challenging to measure Met- and Leu-Enk selectively and independently *in vivo*; in

36 fact, both peptides are typically referred to as ‘enkephalins’, which oversimplifies their distinct
37 properties. Though antibody-based techniques [6–8] or liquid chromatography/mass spectrometry (LC-
38 MS) [9–12] have improved Met- and Leu-Enk detection somewhat, limitations such as spatiotemporal
39 restrictions and poor selectivity between enkephalins remain. Our group previously improved real time
40 *in vivo* detection of evoked opioid peptide release using microdialysis/nanoLC-MS (nLC-MS) after
41 photostimulation [13]. From this strong foundation, we have now optimized a novel opioid peptide
42 detection technique. For the first time, we are able to selectively measure real-time *in vivo* levels of
43 basal peptide release as well as during behavioral manipulations. Our primary goals in establishing this
44 analytical workflow to measure opioid peptide dynamics *in vivo* were to 1) increase temporal resolution
45 allowing for the detection of dynamic changes to short external stimuli and acute conditions, 2) lower
46 the detection threshold to allow for accurate measurements from small brain regions and using less
47 volume of sample, 3) measure endogenous release of peptides in the native state without the need for
48 photo- or chemogenetic stimulation. To meet these goals and measure both Leu- and Met-Enk we used
49 an improved and specialized microdialysis technique coupled with nLC-MS.
50
51 Our workflow (**Fig 1a**) starts with stereotaxic surgery to implant the microdialysis probe in the mouse
52 nucleus accumbens shell (NAcSh). Along with others, we have shown that the opioid receptor system in
53 the NAcSh mediates both reward and aversion through photostimulation of peptide-expressing neurons
54 across the dorsal/ventral axis [14–20]. Our aim was to measure NAcSh peptide release in response to
55 aversive, stressful stimuli. We use custom-made microdialysis probes that are similar in size to commonly
56 used fiber photometry probes to avoid extensive tissue damage caused by traditional microdialysis
57 probes (**Suppl. Fig. 1a**). After recovery, we begin microdialysis collection every 13 minutes, circulating
58 artificial cerebrospinal fluid (aCSF) and collecting interstitial fluid (ISF) at a flow rate of 0.8 μL/min. After
59 each sample collection, we add a consistent known concentration of isotopically labeled internal standard
60 of Met-Enk and Leu-Enk to the collected ISF for the accurate identification and quantification of
61 endogenous peptide. These internal standards have a different mass/charge (m/z) ratio than endogenous

62 Met- and Leu-Enk. Thus, we can identify true endogenous signal for Met-Enk and Leu-Enk (**Suppl Fig.**
63 **2a,c**) versus noise and interfering signals (**Suppl. Fig. 2b,d**). Importantly, we have resolved one of the
64 main barriers preventing the accurate quantification of Met-Enk: the variable oxidation of the methionine
65 residue during sample processing, which results in the signal for Met-Enk being split among multiple m/z
66 values thereby impairing sensitivity. In order to ensure that the signal for Met-Enk is represented by a
67 single m/z value, we converted all methionyl residues to the doubly oxidized sulfone prior to nLC-MS
68 analysis, which allows us to reliably quantify Met-Enk and differentiate it from Leu-Enk [21]. Beyond opioid
69 peptides, this approach represents a key advance and can be applied to any peptide containing a
70 methionine residue. As seen in **Suppl. Fig. 2e**, before the methionine oxidation reaction, Met-Enk can
71 be observed in unoxidized, and singly- and doubly-oxidized forms with varying intensities. However, after
72 the reaction is complete, Met-Enk is observed as doubly oxidized with much higher intensity enabling
73 accurate quantification (**Suppl. Fig. 2f)**. To increase the signal to noise ratio, we also performed solid-
74 phase extraction after the oxidation reaction which removes any salt from the collected samples. To
75 determine the lower limit of quantification (LLOQ), forward and reverse curves were created using varying
76 concentrations of the Met- and Leu-Enk standards in accordance with Clinical Proteomics Tumor Analysis
77 Consortium (CPTAC) guidelines [22]. We determined that the lower limit of quantification (LLOQ), for
78 both Met-Enk and Leu-Enk is 40 amol/sample (**Figure 1b-c**). The improved quantification limit means
79 increased temporal resolution. We now need less volume, (10 μL or less), and shorter sampling times:
80 10 minutes or less, rather than 15-20 minutes as compared to previous studies [13,23]. To test the utility
81 of the method in measuring real-time changes in peptide levels *in vivo*, we evoked the release of the
82 peptides using high $K^+$ ringer's solution, which depolarizes the cells and causes the release of dense
83 core vesicles containing neuropeptides [24]. This depolarization state significantly increased the release
84 of Met- and Leu-Enk in the NAcSh **Figure 1d**. We then quantified the ratio of the Met- to Leu-Enk after
85 applying high K+ solution and showed that this ratio is 3:1 in the NAcSh (**Fig. 1e-f**). The release of Met-
86 Enk is postulated both in vitro and ex vivo to be between 3 to 4 times that of Leu-Enk [25–27]. We are
87 the first to not only corroborate the predicted ratio *in vivo,* but specifically in the NAcSh. Interestingly, this

88 3:1 ratio is almost identical to that previously reported in homogenized human tissue from the
89 sympathoadrenal systems using radioimmunoassays [28]. Importantly, this conserved ratio highlights the
90 usefulness of rodent models for investigating the highly conserved opioid system and demonstrates its
91 potential in translation to humans.
92
93 To highlight the applicability and value of this improved approach, we investigated the changes in the
94 levels of enkephalins following acute stress. It has been hypothesized that enkephalins act as anti-stress
95 signals based on studies that have shown increased preproenkephalin transcript levels following acute
96 stress [29–32]. Moreover, decreased enkephalin expression in the NAc was correlated with an increase
97 in the susceptibility to social defeat [33]. Our group has also recently demonstrated that the
98 photostimulation of peptidergic neurons in the ventral NAcSh drives aversion [14], which further suggests
99 a role for neurons in the NAcSh during aversive stimuli such as stress. Despite the wealth of data
100 implicating these peptides in the stress response, it has not been possible to measure the dynamics of
101 real-time peptide release in response to acute stressful stimuli. We sought to test the hypothesis that
102 Met- and Leu-Enk are released in the NAcSh following acute stress. Using the nLC-MS detection method,
103 we successfully monitored dynamic changes of Met- and Leu-Enk during two different stressors. The first
104 stressor was defined as experimenter handling, which involves the experimenter scruffing the mouse and
105 connecting the inlet tubing and outlet tubing of the microdialysis setup to the microdialysis probe
106 implanted in the mouse brain (**Fig. 1a**). The second stressor was exposure to predator odor (i.e., fox
107 urine). We show that both Met- and Leu-Enk are released following experimenter handling, and that the
108 levels decrease within minutes after exposure to the stress (**Fig. 2a**). We also analyzed the data with sex
109 as a main effect and did not find any differences between males and females after correcting for multiple
110 comparisons (**suppl. Fig. 3a**). We corroborate our finding from **Fig. 1e-f** showing that the ratio of 3:1
111 Met-Enk to Leu-Enk holds following experimenter handling (**Fig. 2c**). Another key finding is that peptide
112 release appears to be precisely controlled. We show that the amol/sample of Met-Enk released at the
113 beginning of the experiment is predictive of later release. For example, a higher level released (in the

fmol/sample range) during the first collections results in lower levels released (in the amol/sample range) during later collections and vice versa (**Fig. 2d**). We show a negative correlation (~ -0.3) between the first two samples (~26 minutes) and the later timepoints, samples 3-10 (~104 minutes). Importantly, this relationship is not due to Met-Enk depletion as the circulation of high K+ aCSF is sufficient to drive the release of Met-Enk at the end of an experiment and reverse the negative correlation (**Fig. 2e**).

To test whether our findings regarding peptide release correlated with neuronal activity following the same stressor, we also monitored enkephalinergic neuron activity using fiber photometry following experimenter handling. To do this, we stereotaxically injected a Cre-dependent adeno-associated virus containing the calcium sensor GCaMP6s in the NAcSh of preproEnkephalin-Cre (pEnk-Cre) mice and implanted fiber photometry probes (**Fig. 2f**). During handling, we observed increased calcium activity in enkephalinergic neurons, even after it was repeated twice within a few minutes (**Fig. 2g**). Individual responses to experimenter handling varied appreciably, as shown by the heatmaps and bar plots (**Fig. 2h-i**); such variation could be due to slight differences in probe placement (**Suppl. Fig 2c-d**) as peptidergic neurons in the dNAcSh encode reward while neurons in the vNAcSh encode aversion [14,34]. Furthermore, the enkephalin precursor is expressed across the dorsal-ventral axis as shown in the *in situ* hybridization atlas (Allen Brain Institute). The fiber photometry data and peptide release data are concordant, as enkephalinergic neurons are activated following experimenter handling, which drives Met- and Leu-Enk somatodendritic release. Critically, the photometry and peptide release data differ in that repeated neuronal activation may not necessarily lead to repeated peptide release, as suggested by the decrease in peptide release over time in **Fig. 2d**. Additionally, fiber photometry cannot provide information about Met- and Leu-Enk independently, as it relies on the precursor gene, *penk*. Taken together, our data suggest that coupling fiber photometry results must be coupled with in vivo measurements of neuropeptides to determine release dynamics.

139 Prior reports have shown that predator odor leads to an increase in the expression of the neuronal
140 activation-associated transcription factor fos in enkephalin-positive neurons in different brain regions
141 including the NAcSh [35,36]. Therefore, we sought to determine whether enkephalins are released in the
142 NAcSh following the exposure to fox urine. We first measured calcium activity of enkephalinergic neurons
143 using fiber photometry after the exposure to fox urine (**Fig. 3a**). We show that upon first exposure, the
144 activity of enkephalinergic neurons increases markedly (**Fig. 3b-d**). However, this enkephalinergic activity
145 is significantly attenuated during second and third exposures that are separated by a few minutes
146 suggesting habituation to the stimulus (**Fig. 3b-d**). We also wondered whether the response to fox urine
147 was also due to the weigh boat used to introduce the fox urine, as it represents a novel object in the
148 home cage, which could be stressful. Using fiber photometry, we measured enkephalinergic calcium
149 activity after introducing a weigh boat containing water to the home cage (**suppl. Fig. 4a**). Interestingly,
150 our data suggest that enkephalinergic neurons also respond to the introduction of a novel object, and the
151 response to the water-containing weigh boat is attenuated upon repeated exposure, which is what we
152 observed for fox urine (**Suppl. Fig. 4b-d**). We compared the enkephalinergic neuron activation in
153 response to both water and fox urine for each individual mouse that experienced both. We see similar
154 calcium transient responses to both the introduction of a novel object and the odor of a predator,
155 suggesting the same subpopulation of enkephalinergic neurons may have been activated (**Suppl Fig.
156 4e**). Interestingly, only recently have researchers shown that a higher level of spiking in the striatum is
157 not always reflected in greater photometry transients. In the future, it will be important to determine
158 whether the fox urine response indeed shows higher action potential spiking than the weigh boat with
159 water [37]. Although the calcium responses to both the fox-urine and water-containing weigh boats were
160 similar in magnitude, it may be that different subpopulations of enkephalinergic neurons are activated in
161 the NAcSh. Further exploration of the specific neurons that respond to the introduction of a novel object
162 or the odor of a predator is warranted. We concluded that enkephalinergic neurons respond to predator
163 odor and novel object introduction; therefore, we tested whether enkephalinergic neuron activation leads
164 to Met- and Leu-Enk release in the NAcSh following predator odor exposure (**Fig. 3e**). In this separate

group of animals, we show that there is a significant increase in Met-Enk release (**Fig. 3f**). The response to predator odor varies appreciably: although most animals show increased Met-Enk release, some show continued release with no elevation in Met-Enk levels, and a minority show no release (**Fig. 3g**). Enkephalins are thought to mediate resilience to stress, so the individual differences in responses to predator odor may indicate differences in stress adaptability [32,38–40]. Moreover, no sex differences in the responses to fox urine were observed, similar to responses to experimenter handling (**Suppl. Fig. 3b**). It is also worth noting that we only observed Leu-Enk release in 3 of 16 experiments. This is likely due to Leu-Enk not being released following predator odor or because it is released at a level below the LLOQ, as suggested by the observed 3:1 ratio of Met-Enk to Leu-Enk (**Fig. 3g**).

In summary, this work allows for multiple unique advances in studying endogenous opioids and neuropeptides in general. First, we have developed a method of methionine stabilization that is transferrable to other neuropeptides and have decreased the LLOQ and temporal resolution. Second, we quantified the relationship between Leu- and Met-Enk and offer a definitive *in vivo* ratio that has long been in question; this ratio corroborates human data and suggests that mice are a useful model system for the study of enkephalinergic release dynamics. Third, we identify a role for the NAcSh in the acute stress response, which has been suggested by studies showing changes in transcript levels of the precursor molecule of enkephalins [33,41]. Fourth, when a limited amount of peptide is released over time, we show that peptide release is biologically constrained and can be experimentally driven using high K+ buffer or photo or chemogenetic stimulation [13]. Finally, we show that Met- and Leu-Enk are released during acute stress, offering evidence for their role in gating the stress response [32]. We also show that data from fiber photometry corroborate peptide release data; however, fiber photometry does not offer the necessary specificity to correlate activation with release, or the distinction between different peptides that arise from the same precursor molecule. Furthermore, this method can immediately be applied to Met- and Leu-Enk samples from other species – enabling the detection of these endogenous opioids in human CSF samples.

**Figures and Legends**:

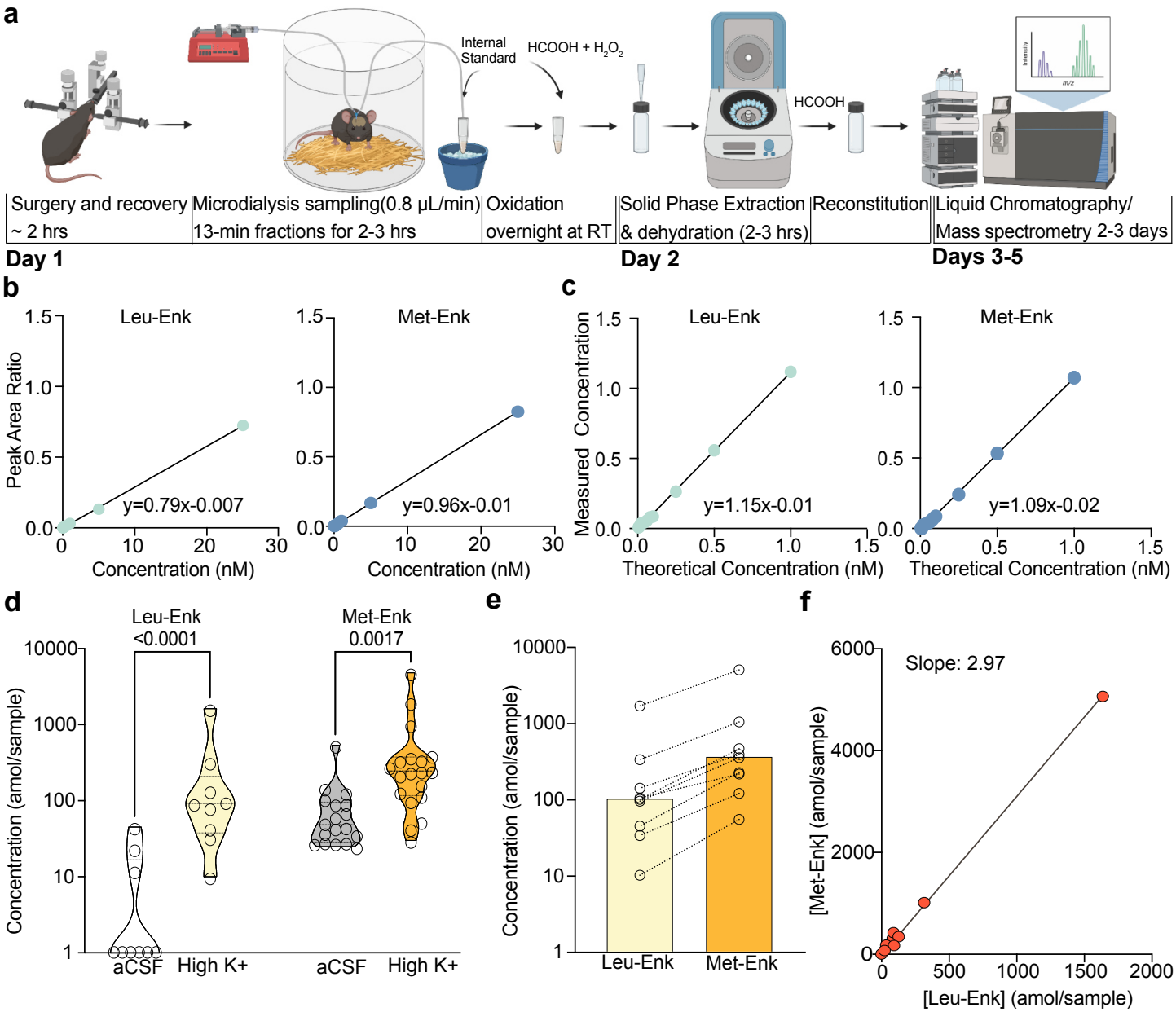


**Figure 1: An optimized approach for *in vivo* Met- and Leu-Enk measurement**. **a.** Timeline of *in vivo* sample collection on day 1 and methionine oxidation reaction overnight, sample processing on day 2, and data acquisition on the LC-MS, days 3-5. The microdialysis probe is implanted via stereotaxic surgery in the ventral Nucleus Accumbens Shell. The mouse is allowed to recover before being connected to the microdialysis lines. Samples are then collected at a rate of 0.8 µL/min for 13 minutes each. After collection is completed, the samples are oxidized overnight. On day 2 the samples undergo solid phase extraction (SPE) and are then dehydrated and reconstituted using formic acid (HCOOH) before being acquired on the LC-MS. **b**. Forward curves of Leu-Enk and Met-Enk showing the peak area ratios as the light standard levels are varied. **c**. Reverse curve of Leu-Enk and Met-enk showing the relationship between the heavy standard concentration applied and the measured concentration based on the instrument. **d.** Violin plots showing that high K+ ringer's solution increases the release of both Leu-Enk and Met-Enk compared to

baseline levels in artificial cerebrospinal fluid (aCSF) (Leu-Enk n=9, Met-Enk n=18). The dashed line indicates the median. **e.** The evoked concentrations of Met-Enk to Leu-Enk in the same samples show that Met-Enk is consistently released at a higher level than Leu-Enk (n=9). **f.** Met-Enk is released at a factor of 2.97 that of Leu-Enk as shown by linear regression analysis of the data in f, suggesting a linear relationship between the two peptides. Data in **d**, **e**, and **f** are transformed to a log scale. In **d**, 2-way ANOVA analysis shows a main effect of peptide, solution, and interaction. The *p*-values reported were calculated using a Sidak's multiple comparisons test.

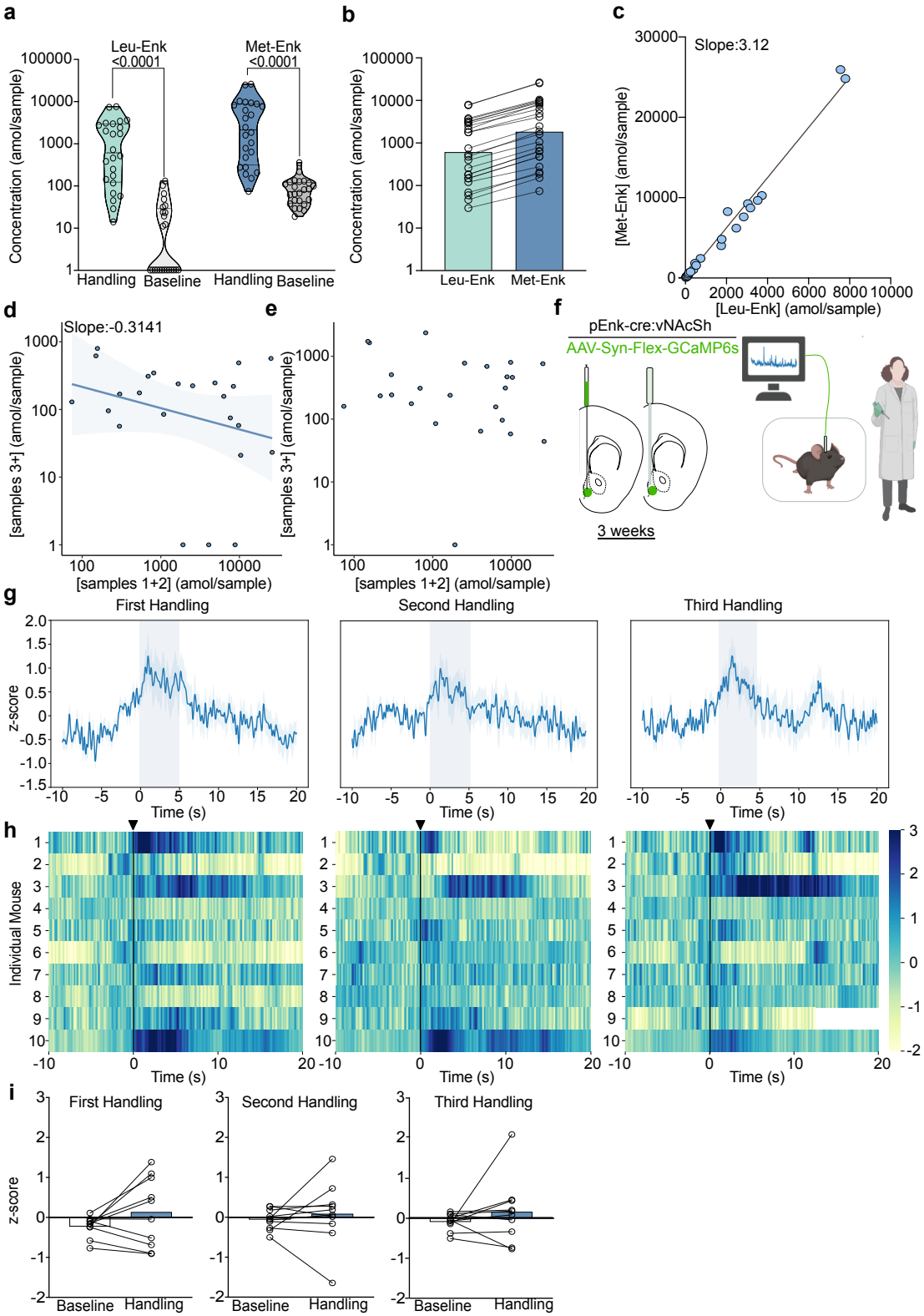


**Figure 2: Experimenter handling evokes the release of Met- and Leu-Enk in the NAcSh. a.** Experimenter handling during microdialysis causes a significant increase in the release of Leu- and Met-Enk in comparison to baseline. **b.** During experimenter handling, Met-Enk is consistently released at a higher rate than Leu-Enk in the same samples. **c.** Linear regression analysis of the data in **b** shows that

Met-enk is released at a rate of 3.12 times the rate of Leu-Enk during experimenter handling suggesting a linear relationship between the two peptides. **d.** A negative correlation (-0.3141) shows that if a high concentration of Met-Enk is released in the first two samples, the concentration released in later samples is affected; such influence suggests that there is regulation of the maximum amount of peptide to be released in NAcSh. **e.** The negative correlation in panel d is reversed by using high K+ buffer to evoke Met-Enk release, suggesting that the limited release observed in **d** is due to modulation of peptide release rather than depletion of reserves. Data in **a-e** are transformed to a log scale and n=24 animals. In panel **a**, 2-way ANOVA analysis shows a main effect of peptide, treatment, and interaction. The *p*-values reported were calculated using a Sidak's multiple comparisons test. **f.** Schematic describing the viral strategy and probe placement for the fiber photometry experiment in pEnk-Cre mice injected with the calcium sensor GCaMP6s in the NAcSh. **g.** Average z-score trace following the first, second, and third events involving experimenter handling. **h**. Heatmaps showing individual mouse z-scored fiber photometry responses before and after experimenter handling. **i**. Bar graphs showing the averaged z-score responses before experimenter handling and after experimenter handling (n=10 for **g-i**).

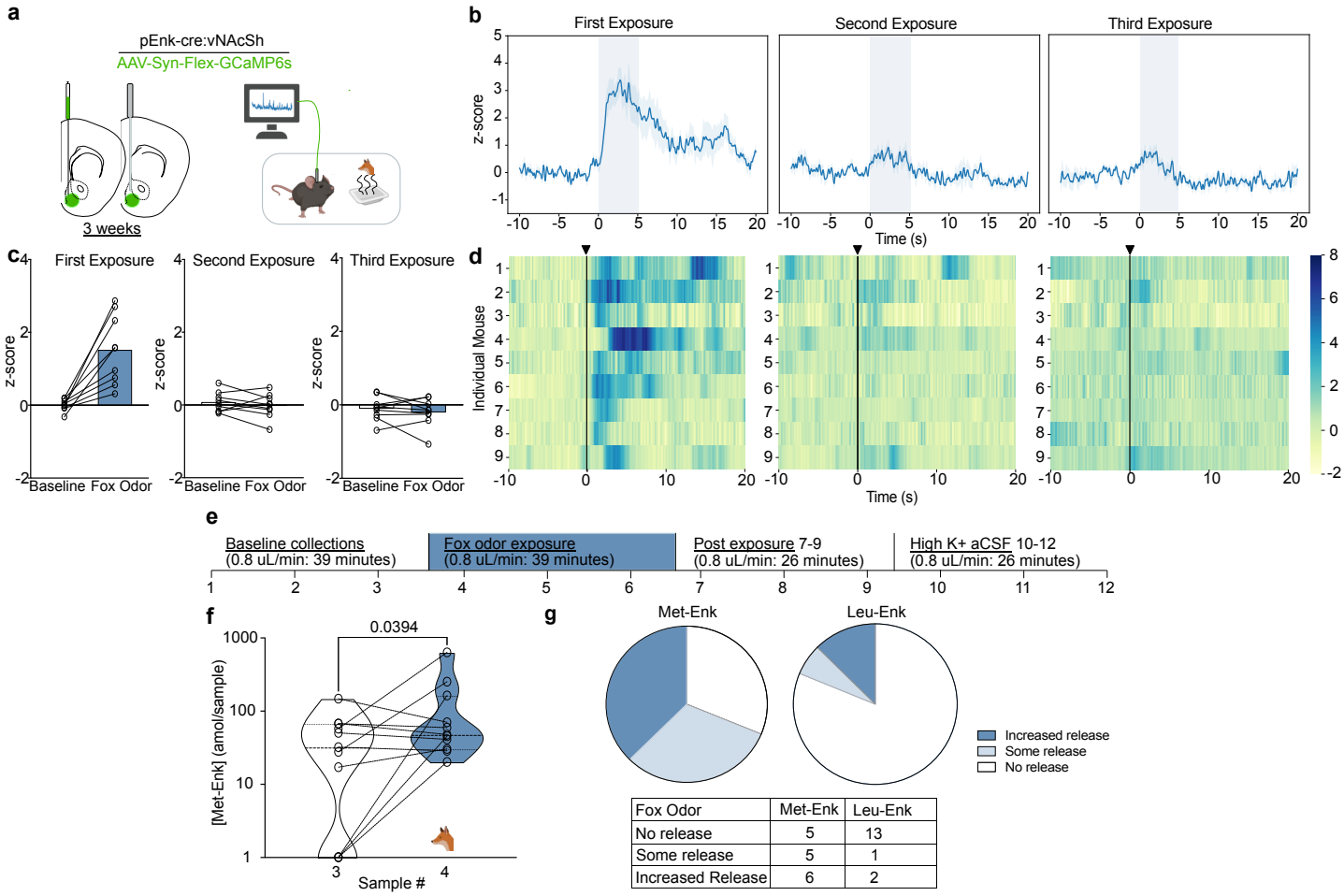


| Fox Odor | Met-Enk | Leu-Enk |
|---|---|---|
| No release | 5 | 13 |
| Some release | 5 | 1 |
| Increased Release | 6 | 2 |

**Figure 3. Fox odor exposure activates enkephalinergic neurons and drives the release of Met-Enk in the NAcSh. a**. Viral strategy and probe placement for the fiber photometry experiment in pEnk-Cre mice injected with the calcium sensor GCaMP6s in the NAcSh. **b.** Averaged z-score traces of the first, second, and third exposure to fox odor. **c.** Bar graphs showing the averaged z-scored fiber photometry responses before and after exposure to fox odor **d**. Heatmaps showing individual mouse z-scored fiber photometry responses before and after exposure to fox odor. (n=9, for **a-d**) **e**. Experimental timeline describing the fox odor microdialysis experiment. **f**. There is a significant increase in Met-Enk concentration during fox odor exposure (sample 4), in comparison to sample, 3 before odor exposure. Data is transformed to a log scale and the *p*-value was calculated using a paired t-test (n=11). **g.** Heatmaps showing the variation in Met-Enk and Leu-Enk release profiles in response to exposure to fox odor, suggesting that such exposure selectively causes the release of Met-Enk but not Leu-Enk in most experiments.

**Materials and Methods:**

**List of Abbreviatons:**

FA, formic acid
MeCN, acetonitrile
MeOH, methanol
DIA, Data-Independent Acquisition
AGC, Automatic Gain Control
*nano*-LC-MS, capillary liquid chromatography interfaced to a mass spectrometer
MS1, mass spectra of peptide precursors
MS2, fragmentation mass spectrum of peptide from precursor ion

**Reagents**

Acetonitrile (MeCN; J.T. Baker, cat. no. 9829-03)

Water (J.T. Baker, cat. no. 4218-03)

Formic Acid (FA; Sigma-Aldrich, cat. no. 56302)

Hydrogen Peroxide (Fisher Chemical, cat. no. H325-100)

Methanol (MeOH; Fluka, cat. no. 34966)

**Equipment**

Stage tips

Laboratory pipetting needles with 90° blunt ends, 16-gauge, 2-inch length; Cadence Science, cat. no. 7938)

C18 extraction disks, diam. = 47 mm, 20 pack; (Empore, cat. no. 66883-U)

Adapter for stage tipping (Glygen, cat. no. CEN.24)

1.5-ml tubes (Axygen, Cat. No. MCT-175-C)
Eppendorf centrifuge (Eppendorf, model 5424R)

Vortex (Labnet VX100)

Autosampler vials (Sun-Sri, Cat. No. 200046)

Autosampler vial caps (Sun-Sri, cat. no. 501 382)

UPLC system for LC-MS of analysis of TMT-labeled peptides (EASY nL-LC 1000, Thermo Scientific)

Mass spectrometer for analysis of TMT-labeled peptides (Q-Exactive™ Plus Hybrid Quadrupole Orbitrap™, Thermo Scientific)

EASY-Spray™ column, 75 µm x 50 cm PepMap (Thermo Scientific™, cat. no. ES903)

**Animals**

Adult male and female C57BL/6 mice at 8-15 weeks of age were used for microdialysis procedures. For fiber photometry, adult preproEnkephalin-Cre (pEnk-Cre) male and female mice at ages between 15-24

285 weeks of age were used to measure enkephalinergic cell activity. Mice were group housed and kept at
286 a 12-hour light/dark cycle with *ad libitum* access to water and food. The holding facility was both
287 temperature and humidity controlled. All surgical and behavioral procedures were approved by the
288 Washington University School of Medicine animal care guidelines in accordance with federal animal
289 use regulations.

290 **Chemicals**

291 Met and Leu Enkephalin standards including isotopically labeled forms were synthesized at New
292 England Peptide and can be ordered by the research community. The heavy isotope labeled Leu
293 Enkephalin is synthesized with a fully labeled L-Leucine ($^{13}C_6$, $^{15}N$) at the C terminus of the peptide
294 (YGGF**L**). For Met Enkephalin, a fully labeled L-Phenylalanine ($^{13}C_9$, $^{15}N$) was added (YGG**F**M). The
295 resulting mass shift between the endogenous (light) and heavy isotope-labeled peptide are 7Da and
296 10Da, respectively. Heavy isotope amino acids are guaranteed >99% pure. Peptide purity
297 specifications are set at ≥ 95% pure by area on a regular HPLC gradient with UV detection. Artificial
298 cerebrospinal fluid (aCSF) contained 124 mM NaCl, 2.5 mM KCl, 2 mM $CaCl_2$, 1 mM $MgCl_2$, 1.25 mM
299 $NaH_2PO_4$, 24 mM $NaHCO_3$, 5 mM HEPES, 12.5 mM Glucose adjusted to pH 7.4 with NaOH. High $K^+$
300 ringer solution contained 48 mM NaCl, 100 mM KCl, 2.4 mM $CaCl_2$, 0.85 mM $MgCl_2$ adjusted to pH 7.4
301 with NaOH as described in (Al-Hasani, 2018). All salt compounds were purchased from Sigma (St.
302 Louis, MO).

303 ***In vivo* microdialysis**

304 Custom microdialysis probes (BASI Inc. part MD-2206) of 5 mm shaft length and 1 mm Polyacrylonitrile
305 membrane with a 30 kDa molecular weight cutoff were used for the *in vivo* experiments. The probes
306 were flushed prior to surgical implantation for 15 minutes at 10 μL/min with artificial cerebrospinal fluid
307 as directed by the manufacturer using a BASI syringe pump (MD 1001). For the surgical procedure,
308 mice were briefly anaesthetized in an induction chamber at 3% isofluorane before being placed in a
309 stereotaxic frame (Kopf) secured with ear and bite bars. During the surgery, the isofluorane level was
310 kept at 1.5-2%. The probe was then inserted into the ventral Nucleus Accumbens shell (stereotaxic

311 coordinates from bregma: +1.3 [AP], ±0.5 [ML], −5.0 mm [DV]). Implanted probes were secured with
312 dental adhesive (C&B metabond kit) followed by cyanoacrylate (Loctite superglue gel control).
313 After the completion of the surgery, each mouse was allowed to recover for 30 minutes. The mouse
314 was then connected to an inlet perfusion line to circulate aCSF or high K+ ringer solution and an outlet
315 perfusion line to collect the interstitial fluid from the NAcSh. The outlet line directly collected sample in a
316 tube that is kept at 4 °C throughout the experiment. The flow of aCSF was then then turned on and
317 sample collection time started as sample began to collect in the outlet tube. The flow rate of aCSF was
318 set to 0.8 μL/min during sample collection. Fractions were collected every 13 minutes resulting in a 10
319 μL sample. After each collection, the samples were spiked with 2 μL of 12.5 fM isotopically labeled Met-
320 Enkephalin and Leu-Enkephalin. The microdialysis rig (BASI Raturn MD 1404) was equipped with
321 bedding, regular mouse chow and water ad libitum. While connected to the perfusion lines, the mice
322 were allowed to move freely. For the experiments measuring evoked release, the high K+ ringer
323 solution was perfused through the lines instead of aCSF at 0.8 μL/min and fractions were collected
324 every 13 minutes as described previously. The samples were similarly spiked with 2 μL of 12.5 fM
325 isotopically labeled Met-Enkephalin and Leu-Enkephalin.
326 For the experiments where the animals were exposed to the fox urine odor, 3 mL of fox urine was
327 absorbed into a kim wipe contained in a chemical weigh boat. The weigh boats were prepared and
328 remained in a fume hood the experiment to prevent the odor permeating the experimental space before
329 the planned collection. Then, the experimenter placed the weigh boat in the microdialysis rig and
330 allowed the mouse to explore it. The exposure was standardized to span 3 fractions (39 minutes)
331 during each of the experiments while aCSF was being perfused through the lines.

332 **In vivo sample processing**

333 ***Methionine Oxidation Reaction***

334 For met-enkephalin detection and stabilization, the animal samples underwent a methionine oxidation
335 reaction [21]. To each sample vial, 28 μl of 0.1% (vol/vol) formic acid (FA) was added and then the

336 samples were transferred to 0.5 mL tubes from the collection tubes. Afterwards, 40 μl of a mixture of
337 6% FA (vol/vol) and 6% hydrogen peroxide (vol/vol) was added to each of the sample tubes and mixed
338 and gently spun. The samples were then incubated overnight at room temperature.

339 ***Solid Phase Extraction with C18 stage tips***

340 After the methionine oxidation reaction, a solid phase extraction process was performed using C18
341 stage tips. Stage tips were conditioned before sample loading. To each of the stage tips, 100 μl of
342 methanol is added and then spun for 2 minutes at 2,000 rpm in microcentrifuge tubes. The stage tips
343 were then rinsed with 100 μl of a mixture of 50% acetonitrile (MeCN; (vol/vol)) and 0.1% FA (vol/vol)
344 followed by a 2-minute spin at 2,000 rpm. This was followed by a rinse in 0.1% FA (vol/vol) and a 2-
345 minute spin at 3,000 rpm. The final rinse was done by adding 100 μl of 1% FA (vol/vol) to each of the
346 stage tips. Following the final rinse, the samples were added to the C18 stage tips and spun for 10
347 minutes at 0.8 rpm. After ensuring that the samples passed through the stage tips, the samples were
348 desalted with 0.1% FA (vol/vol) and spun for 1.5 minutes at 3,000 rpm twice. After the spins were done,
349 the stage tips were directly placed into autosampler vials to elute the analyte with 60 μl of 50% MeCN,
350 0.1% FA (vol/vol) using a syringe. Eluates in the autosampler vial were dried in a speedvac,
351 reconstituted in 3 μl 1% FA (vol/vol) and set up on the autosampler for injection on the mass
352 spectrometer.

353 ***Nano*-LC-MS/MS.** The samples in formic acid (1%) were loaded (2.5 μl) onto a 75 μm i.d. × 50 cm
354 Acclaim® PepMap 100 C18 RSLC column (Thermo-Fisher Scientific) on an EASY *nano*LC (Thermo
355 Fisher Scientific) at a constant pressure of 700 bar at 100% A (1%FA). Prior to sample loading the
356 column was equilibrated to 100%A for a total of 11 μL at 700 bar pressure. Peptide chromatography
357 was initiated with mobile phase A (1% FA) containing 5%B (100%MeCN, 1%FA) for 1 min, then
358 increased to 20% B over 19 min, to 32% B over 10 min, to 95% B over 1 min and held at 95% B for 19
359 min, with a flow rate of 250 nL/min. The data was acquired in data-independent acquisition (DIA) mode.
360 The full-scan mass spectra were acquired with the Orbitrap mass analyzer with a scan range of *m/z* =

361 150 to 1500 and a mass resolving power set to 70,000. Data-independent (DIA) high-energy collisional
362 dissociations were performed according to the inclusion list with a mass resolving power set to 17,500,
363 an isolation width of 2 Da, and a normalized collision energy setting of 27. The maximum injection time
364 was 60 ms for parent-ion analysis and product-ion analysis. The automatic gain control (AGC) was set
365 at a target value of 3e6 ions for full MS scans and 2e5 ions for MS2. The inclusion list contained 4
366 peptide entries. The loop count was set at 30. Retention time windows were set at 20 min.

367 **Stable-isotope dilution assay for measurement of enkephalins**

368 Peptides were synthesized as high purity natural abundance and stable isotope-labeled pairs. Assays
369 were developed as Tier 2 assays according to CPTAC guidelines [22]. Co-eluting peak boundaries for
370 the internal standard and endogenous peptides were manually refined using the Skyline software
371 package [42]. Integrated peak areas for the three most intense fragment ions were then exported for
372 determination of peak area ratios of endogenous to internal standard signal, which were used as a
373 basis for determining abundance and quantifying changes in enkephalin levels in mouse studies.

374 ***In vivo* fiber photometry**
375
376 Stereotaxic surgery

377 For the surgical procedure, pEnk-Cre mice were briefly anaesthetized in an induction chamber at 3%
378 isofluorane before being placed in a stereotaxic frame (Kopf) secured with ear and bite bars. During the
379 surgery, the isofluorane level was kept at 1.5-2%. Then we performed a craniotomy and unilaterally
380 injected using a Nanoject III (Drummond) 200-250 nL of AAV5.Syn.Flex.GCaMP6s.WPRE.SV40
381 (Addgene: 100845-AAV5) at the following coordinates :+1.3 [AP],±0.5 [ML], −5.0 mm [DV]. To allow for
382 viral expression, the fiber photometry probes (5 mm shaft length, doric lenses) were implanted 3 weeks
383 later at +1.3 [AP], ±0.5 [ML], −4.75 mm [DV]. Implanted probes were secured with dental adhesive
384 (C&B metabond kit) followed by cyanoacrylate (Loctite superglue gel control).

385 Fiber photometry recording procedure

386 Before recording, the implanted probes were tethered to an optic fiber using a ferrule sleeve (Doric,
387 catalog no. ZR_2.5). Two light-emitting diodes (LEDs) were used to excite GCaMP6s. A 331 Hz

388 sinusoidal LED light (Doric) of wavelength 470 nm 470 ± 20 nm was used for the $Ca^{2+}$ -dependent
389 signal. A 210 Hz sinusoidal LED light of wavelength 405 ± 10 nm (Doric, LED driver) was used to evoke
390 the $Ca^{2+}$ -independent signal and serve as the isosbestic control. GCaMP6s fluorescence traveled
391 through the same optic fiber before being bandpass filtered (525 ± 25 nm, Doric, catalog no. FMC4),
392 transduced by a femtowatt photoreceiver (New Focus Model 2151) and recorded by a real-time
393 processor (TDT, RZ5P). The signals were extracted by the Synapse software (TDT). During the
394 recording, two behavioral manipulations were introduced. The first was after a 10-minute recording in a
395 home cage environment, an experimenter handled the mouse while the recording was ongoing. The
396 mouse was then let go and the handling was repeated another two times in a single session. The
397 second behavioral manipulation was introduced to the same mice a week after the first recording
398 session. After a 10-minute recording in the home cage environment, a weight boat containing a kim
399 wipe that had absorbed 3 mL of fox urine was placed in the cage as the recording proceeded. The
400 weigh boat was removed after a couple of minutes of exploration then re-introduced into the cage for
401 another two times during the session.

402 Fiber Photometry Data Analysis

403 Data analysis was performed through the python toolbox GuPPy [43]. Briefly, the isosbestic control
404 signal was used to correct for motion and photobleaching artifacts. The control channel is fitted to the
405 signal channel using a least squares polynomial fit of degree 1. Transient detection occurred after using
406 a 15s moving window for thresholding transients. Then, high-amplitude events were identified and their
407 timestamp of occurrence during the session was reported. To determine the effect of handling or fox
408 urine exposure on enkephalinergic cell activity, the event timestamp was used to observe changes in
409 activity before and after the behavioral manipulation. The average of all trials is then calculated for
410 repeated exposures and for exposures in multiple animals. The fiber photometry data was represented
411 as z-scores.

412 Immunohistochemistry and verification of probe placement

After the completion of the experiment, mice were anaesthetized with a mixture of ketamine, xylazine and acepromazine and transcardially perfused with ice-cold 4% paraformaldehyde in phosphate buffer. After the perfusion, brains were dissected and fixed for 24 hours in 4% paraformaldehyde at 4°C and then placed in 30% sucrose solution for cryoprotection for a minimum of 48 hours. The brains were then sliced into 30 um sections, washed three times in PBS and blocked in PBS containing 0.5% Triton X-100 and 5% goat serum for one hour. Following the blocking step, the slices were stained for the glial fibrillary acidic protein (GFAP), an astrocyte marker to determine glial scarring around the probe site (guinea pig anti-GFAP, synaptic systems) at 1:500 dilution and incubated at 4°C for 16 hours. The next day, the sections were washed three times with PBS and stained with the secondary antibody, mouse anti-guinea pig, Alexa Fluor 594 (Invitrogen) at 1:500 dilution and incubated for two hours at room temperature. After the incubation, the slices were washed three times in PBS, followed by two washes with PB. Finally, the slices were mounted on glass slides with Hard set Vectashield with DAPI staining (Vector Labs) and imaged using an epifluorescence microscope (Leica DM6 B). Correct probe placement in the NAcSh is represented in **supplementary figure 1b**.

For the verification of the injection and probe placement for fiber photometry, the same procedure described above was performed for tissue preparation. After slicing, the slices were washed in a 0.1% Triton for one hour in order to permeabilize the cells followed by two 10-minute PBS washes. The slices were then stained with Neurotrace (Nissl) red (Invitrogen) to mark neurons by adding 5 μL to each well for 2 hours at room temperature followed by 3 10-minute PBS washes and 3 10-minute PB washes. Finally, the slices were mounted using Hard set Vectashield (Vector Labs). GCaMP6s expression was determined by observing green fluorescent protein expression colocalized with Neurotrace staining. Correct probe placement in the NAcSh is represented in **supplementary figure 1d**.

**Funding**

This work was supported by National Institutes on Drug Abuse R00 DA038725 (RA) and R21DA048650 (RA). The NARSAD Young Investigator Grant from the Brain and Behavior Research Foundation, grant

no. 28243 (RA). The WU-PSR is supported in part by the WU Institute of Clinical and Translational Sciences (NCATS UL1 TR000448), the Mass Spectrometry Research Resource (NIGMS P41 GM103422; R24GM136766) and the Siteman Comprehensive Cancer Center Support Grant (NCI P30 CA091842). Cognitive, Computational, and Systems Neuroscience Fellowship (MOM).

**Author Contributions**

- Marwa Mikati conducted the *in vivo* experiments, analyzed the data, and wrote the manuscript with the assistance and supervision of Robert Sprung PhD, Reid Townsend MD, Ph.D., and Ream Al-Hasani Ph.D.
- Petra Erdmann-Gilmore and Rose Connors processed and analyzed the microdialysis samples for nLC-MS.
- Sineadh Conway, PhD assisted with *in vivo* microdialysis and fiber photometry experiments.
- Jim Malone assisted with proteomic data analysis and visualization.
- Justin Woods assisted with the immunohistochemistry experiments.
- The proteomic experiments were performed at the Washington University Proteomics Shared Resource (WU-PSR), under the supervision and guidance of R Reid Townsend M.D., Ph.D., Director and Robert Sprung, PhD., Co-Director.
- Ream Al-Hasani, PhD conceptualized the study and supervised the experiments.
- All authors assisted with the preparation of the manuscript.

**Acknowledgments**

The figure schematics were created with biorender.com. We would like to thank Justin W. Baldwin for his guidance on appropriate data visualization tools and for his support in proofreading the manuscript. We would also like to thank Dr. Jordan McCall for his advice on data analysis and visualization as well as proofreading the manuscript. Thank you to Emily Wheeler for proofreading the manuscript and providing feedback on sentence structure and flow. We would also like to thank the entirety of the proteomics core team including Dr. Yiling Mi for her assistance. Thank you to the entirety of the Al-

Hasani and McCall labs for their feedback on experimental design and analysis. Finally, thank you to Dr. Tim Holy, Dr. Robyn Klein, and Dr. Alexxai Kravitz for their feedback.

## References


[1] L.D. Fricker, E.B. Margolis, I. Gomes, L.A. Devi, Five Decades of Research on Opioid Peptides: Current Knowledge and Unanswered Questions, Mol Pharmacol. 98 (2020) 96–108. https://doi.org/10.1124/MOL.120.119388.

[2] M.R. Banghart, X.J. He, B.L. Sabatini, A Caged Enkephalin Optimized for Simultaneously Probing Mu and Delta Opioid Receptors, ACS Chem Neurosci. 9 (2018) 684–690. https://doi.org/10.1021/ACSCHEMNEURO.7B00485/ASSET/IMAGES/LARGE/CN-2017-00485A_0003.JPEG.

[3] I. Gomes, S. Sierra, L. Lueptow, A. Gupta, S. Gouty, E.B. Margolis, B.M. Cox, L.A. Devi, Biased signaling by endogenous opioid peptides, Proceedings of the National Academy of Sciences. 117 (2020) 11820–11828. https://doi.org/10.1073/pnas.2000712117.

[4] A. Mansour, M.T. Hoversten, L.P. Taylor, S.J. Watson, H. Akil, The cloned μ, δ and κ receptors and their endogenous ligands: Evidence for two opioid peptide recognition cores, Brain Res. 700 (1995) 89–98. https://doi.org/10.1016/0006-8993(95)00928-J.

[5] M.R. Banghart, S.Q. Neufeld, N.C. Wong, B.L. Sabatini, Enkephalin Disinhibits Mu Opioid Receptor-Rich Striatal Patches via Delta Opioid Receptors, Neuron. 88 (2015) 1227–1239. https://doi.org/10.1016/J.NEURON.2015.11.010.

[6] N.T. Maidment, D.R. Brumbaugh, V.D. Rudolph, E. Erdelyi, C.J. Evans, Microdialysis of extracellular endogenous opioid peptides from rat brain in vivo, Neuroscience. 33 (1989) 549–557. https://doi.org/10.1016/0306-4522(89)90407-7.

[7] P.W. Marinelli, L. Bai, R. Quirion, C. Gianoulakis, A Microdialysis Profile of Met-Enkephalin Release in the Rat Nucleus Accumbens Following Alcohol Administration, Alcohol Clin Exp Res. 29 (2005) 1821–1828. https://doi.org/10.1097/01.alc.0000183008.62955.2e.

[8] L. Hemandez, B.G. Hoebel, Food reward and cocaine increase extracellular dopamine in the nucleus accumbens as measured by microdialysis, 1988.

[9] M.M. Nieto, J. Wilson, A. Cupo, B.P. Roques, F. Noble, Chronic Morphine Treatment Modulates the Extracellular Levels of Endogenous Enkephalins in Rat Brain Structures Involved in Opiate Dependence: A Microdialysis Study, The Journal of Neuroscience. 22 (2002) 1034–1041. https://doi.org/10.1523/JNEUROSCI.22-03-01034.2002.

[10] O.S. Mabrouk, Q. Li, P. Song, R.T. Kennedy, Microdialysis and Mass Spectrometric Monitoring of Dopamine and Enkephalins in the Globus Pallidus Reveal Reciprocal Interactions that Regulate Movement, J Neurochem. 118 (2011) 24. https://doi.org/10.1111/J.1471-4159.2011.07293.X.

[11] Q. Li, Jon-Kar Zubieta, R.T. Kennedy, Practical Aspects of in Vivo Detection of Neuropeptides by Microdialysis Coupled Off-Line to Capillary LC with Multi-stage MS, Anal Chem. 81 (2009) 2242. https://doi.org/10.1021/AC802391B.

[12] H.M. Baseski, C.J. Watson, N.A. Cellar, J.G. Shackman, R.T. Kennedy, Capillary liquid chromatography with MS3 for the determination of enkephalins in microdialysis samples from the striatum of anesthetized and freely-moving rats, Journal of Mass Spectrometry. 40 (2005) 146–153. https://doi.org/10.1002/jms.733.

[13] R. Al-Hasani, J.-M.T. Wong, O.S. Mabrouk, J.G. McCall, G.P. Schmitz, K.A. Porter-Stransky, B.J. Aragona, R.T. Kennedy, M.R. Bruchas, In vivo detection of optically-evoked opioid peptide release, Elife. 7 (2018). https://doi.org/10.7554/eLife.36520.

[14] R. Al-Hasani, J.G. McCall, G. Shin, A.M. Gomez, G.P. Schmitz, J.M. Bernardi, C.-O. Pyo, S. il Park, C.M. Marcinkiewcz, N.A. Crowley, M.J. Krashes, B.B. Lowell, T.L. Kash, J.A. Rogers, M.R. Bruchas, Distinct Subpopulations of Nucleus Accumbens Dynorphin Neurons Drive Aversion and Reward., Neuron. 87 (2015) 1063–77. https://doi.org/10.1016/j.neuron.2015.08.019.

[15] B.E. Pirino, M.B. Spodnick, A.T. Gargiulo, G.R. Curtis, J.R. Barson, A.N. Karkhanis, Kappa-opioid receptor-dependent changes in dopamine and anxiety-like or approach-avoidance behavior occur differentially across the nucleus accumbens shell rostro-caudal axis, Neuropharmacology. 181 (2020). https://doi.org/10.1016/J.NEUROPHARM.2020.108341.

[16] B.H. Trieu, B.C. Remmers, C. Toddes, D.D. Brandner, E.M. Lefevre, A. Kocharian, C.L. Retzlaff, R.M. Dick, M.A. Mashal, E.A. Gauthier, W. Xie, Y. Zhang, S.S. More, P.E. Rothwell, Angiotensin-converting enzyme gates brain circuit–specific plasticity via an endogenous opioid, Science (1979). 375 (2022) 1177–1182. https://doi.org/10.1126/SCIENCE.ABL5130/SUPPL_FILE/SCIENCE.ABL5130_DATA_S1.ZIP.

[17] S.M. Reynolds, K.C. Berridge, Positive and negative motivation in nucleus accumbens shell: bivalent rostrocaudal gradients for GABA-elicited eating, taste “liking”/"disliking" reactions, place preference/avoidance, and fear, J Neurosci. 22 (2002) 7308–7320. https://doi.org/10.1523/JNEUROSCI.22-16-07308.2002.

[18] D.C. Castro, M.R. Bruchas, A Motivational and Neuropeptidergic Hub: Anatomical and Functional Diversity within the Nucleus Accumbens Shell, Neuron. 102 (2019) 529–552. https://doi.org/10.1016/J.NEURON.2019.03.003.

[19] A.G. Schindler, D.I. Messinger, J.S. Smith, H. Shankar, R.M. Gustin, S.S. Schattauer, J.C. Lemos, N.W. Chavkin, C.E. Hagan, J.F. Neumaier, C. Chavkin, Stress produces aversion and potentiates cocaine reward by releasing endogenous dynorphins in the ventral striatum to locally stimulate serotonin reuptake, J Neurosci. 32 (2012) 17582–17596. https://doi.org/10.1523/JNEUROSCI.3220-12.2012.

[20] D.C. Castro, K.C. Berridge, Opioid Hedonic Hotspot in Nucleus Accumbens Shell: Mu, Delta, and Kappa Maps for Enhancement of Sweetness “Liking” and “Wanting,” Journal of Neuroscience. 34 (2014) 4239–4250. https://doi.org/10.1523/JNEUROSCI.4458-13.2014.

[21] J.J. Pesavento, B.A. Garcia, J.A. Streeky, N.L. Kelleher, C.A. Mizzen, Mild performic acid oxidation enhances chromatographic and top down mass spectrometric analyses of histones, Mol Cell Proteomics. 6 (2007) 1510–1526. https://doi.org/10.1074/MCP.M600404-MCP200.

[22] S.A. Carr, S.E. Abbatiello, B.L. Ackermann, C. Borchers, B. Domon, E.W. Deutsch, R.P. Grant, A.N. Hoofnagle, R. Hüttenhain, J.M. Koomen, D.C. Liebler, T. Liu, B. MacLean, D.R. Mani, E. Mansfield, H. Neubert, A.G. Paulovich, L. Reiter, O. Vitek, R. Aebersold, L. Anderson, R. Bethem, J. Blonder, E. Boja, J. Botelho, M. Boyne, R.A. Bradshaw, A.L. Burlingame, D. Chan, H. Keshishian, E. Kuhn, C. Kinsinger, J.S.H. Lee, S.W. Lee, R. Moritz, J. Oses-Prieto, N. Rifai, J. Ritchie, H. Rodriguez, P.R. Srinivas, R.R. Townsend, J. van Eyk, G. Whiteley, A. Wiita, S. Weintraub, Targeted peptide measurements in biology and medicine: Best practices for mass spectrometry-based assay development using a fit-for-purpose approach, Molecular and Cellular Proteomics. 13 (2014) 907–917.

https://doi.org/10.1074/MCP.M113.036095/ATTACHMENT/D53FF2E2-A6B1-4AAD-BC0D-B7F9E6821120/MMC1.PDF.

[23] A.G. Difeliceantonio, O.S. Mabrouk, R.T. Kennedy, K.C. Berridge, Enkephalin surges in dorsal neostriatum as a signal to eat, Current Biology. 22 (2012) 1918–1924. https://doi.org/10.1016/J.CUB.2012.08.014.

[24] T.L. Ripley, J. Jaworski, P.K. Randall, R.A. Gonzales, Repeated perfusion with elevated potassium in in vivo microdialysis - A method for detecting small changes in extracellular dopamine, J Neurosci Methods. 78 (1997) 7–14. https://doi.org/10.1016/S0165-0270(97)00129-5.

[25] M. Comb, P.H. Seeburg, J. Adelman, L. Eiden, E. Herbert, Primary structure of the human Met- And Leu-enkephalin precursor and its mRNA, Nature. 295 (1982) 663–666. https://doi.org/10.1038/295663a0.

[26] J. Hughes, H.W. Kosterlitz, T.W. Smith, The distribution of methionine-enkephalin and leucine-enkephalin in the brain and peripheral tissues, Br J Pharmacol. 120 (1997) 428–436. https://doi.org/10.1111/j.1476-5381.1997.tb06829.x.

[27] G. Henderson, J. Hughes, H.W. Kosterlitz, In vitro release of Leu- and Met-enkephalin from the corpus striatum, Nature 1978 271:5646. 271 (1978) 677–679. https://doi.org/10.1038/271677a0.

[28] T. Yoshimasa, K. Nakao, H. Ohtsuki, S. Li, H. Imura, Methionine-enkephalin and leucine-enkephalin in human sympathoadrenal system and pheochromocytoma, Journal of Clinical Investigation. 69 (1982) 643–650. https://doi.org/10.1172/JCI110491.

[29] J.A. Mansi, S. Laforest, G. Drolet, Effect of stress exposure on the activation pattern of enkephalin-containing perikarya in the rat ventral medulla, J Neurochem. 74 (2000) 2568–2575. https://doi.org/10.1046/J.1471-4159.2000.0742568.X.

[30] E.C. Dumont, R. Kinkead, J.F. Trottier, I. Gosselin, G. Drolet, Effect of chronic psychogenic stress exposure on enkephalin neuronal activity and expression in the rat hypothalamic paraventricular nucleus, J Neurochem. 75 (2000) 2200–2211. https://doi.org/10.1046/J.1471-4159.2000.0752200.X.

[31] S. Ceccatelli, C. Orazzo, Effect of different types of stressors on peptide messenger ribonucleic acids in the hypothalamic paraventricular nucleus, Acta Endocrinol (Copenh). 128 (1993) 485–492. https://doi.org/10.1530/ACTA.0.1280485.

[32] R.J. Valentino, E. van Bockstaele, Endogenous opioids: The downside of opposing stress, Neurobiol Stress. 1 (2015) 23–32. https://doi.org/10.1016/J.YNSTR.2014.09.006.

[33] H. Nam, R. Chandra, T.C. Francis, C. Dias, J.F. Cheer, M.K. Lobo, Reduced nucleus accumbens enkephalins underlie vulnerability to social defeat stress, Neuropsychopharmacology. 44 (2019) 1876–1885. https://doi.org/10.1038/s41386-019-0422-8.

[34] J.W. de Jong, S.A. Afjei, I. Pollak Dorocic, J.R. Peck, C. Liu, C.K. Kim, L. Tian, K. Deisseroth, S. Lammel, A Neural Circuit Mechanism for Encoding Aversive Stimuli in the Mesolimbic Dopamine System, Neuron. 101 (2019) 133-151.e7. https://doi.org/10.1016/J.NEURON.2018.11.005.

[35] A.L.O. Hebb, R.M. Zacharko, M. Gauthier, F. Trudel, S. Laforest, G. Drolet, Brief exposure to predator odor and resultant anxiety enhances mesocorticolimbic activity and enkephalin expression in CD-1 mice, European Journal of Neuroscience. 20 (2004) 2415–2429. https://doi.org/10.1111/j.1460-9568.2004.03704.x.

[36] A. Asok, L.W. Ayers, B. Awoyemi, J. Schulkin, J.B. Rosen, Immediate early gene and neuropeptide expression following exposure to the predator odor 2,5-dihydro-2,4,5-trimethylthiazoline (TMT), Behavioural Brain Research. 248 (2013) 85–93. https://doi.org/10.1016/J.BBR.2013.03.047.

[37] A.A. Legaria, B.A. Matikainen-Ankney, B. Yang, B. Ahanonu, J.A. Licholai, J.G. Parker, A. v. Kravitz, Fiber photometry in striatum reflects primarily nonsomatic changes in calcium, Nature Neuroscience 2022 25:9. 25 (2022) 1124–1128. https://doi.org/10.1038/s41593-022-01152-z.

[38] P. Bérubé, J.F. Poulin, S. Laforest, G. Drolet, Enkephalin Knockdown in the Basolateral Amygdala Reproduces Vulnerable Anxiety-Like Responses to Chronic Unpredictable Stress, Neuropsychopharmacology 2014 39:5. 39 (2013) 1159–1168. https://doi.org/10.1038/npp.2013.316.

[39] P. Bérubé, S. Laforest, S. Bhatnagar, G. Drolet, Enkephalin and dynorphin mRNA expression are associated with resilience or vulnerability to chronic social defeat stress, Physiol Behav. 122 (2013) 237–245. https://doi.org/10.1016/J.PHYSBEH.2013.04.009.

[40] I. Melo, E. Drews, A. Zimmer, A. Bilkei-Gorzo, Enkephalin knockout male mice are resistant to chronic mild stress, Genes Brain Behav. 13 (2014) 550–558. https://doi.org/10.1111/GBB.12139.

[41] A.L.O. Hebb, R.M. Zacharko, M. Gauthier, F. Trudel, S. Laforest, G. Drolet, Brief exposure to predator odor and resultant anxiety enhances mesocorticolimbic activity and enkephalin expression in CD-1 mice, European Journal of Neuroscience. 20 (2004) 2415–2429. https://doi.org/10.1111/j.1460-9568.2004.03704.x.

[42] B. MacLean, D.M. Tomazela, N. Shulman, M. Chambers, G.L. Finney, B. Frewen, R. Kern, D.L. Tabb, D.C. Liebler, M.J. MacCoss, Skyline: an open source document editor for creating and analyzing targeted proteomics experiments, Bioinformatics. 26 (2010) 966–968. https://doi.org/10.1093/BIOINFORMATICS/BTQ054.

[43] V.N. Sherathiya, M.D. Schaid, J.L. Seiler, G.C. Lopez, T.N. Lerner, GuPPy, a Python toolbox for the analysis of fiber photometry data, Scientific Reports 2021 11:1. 11 (2021) 1–9. https://doi.org/10.1038/s41598-021-03626-9.